Capacitance measurements of a quantized two-dimensional electron gas in the regime of the quantum Hall effect

R. K. Goodall, R. J. Higgins, and J. P. Harrang
Physics Department, University of Oregon, Eugene, Oregon 97403-1274
(Received 4 June 1984)

We report measurements and a self-consistent theory of the capacitance oscillations in a two-dimensional electron gas in the quantum-Hall-effect regime. The capacitance shows very strong structure which can be quantitatively explained as a function of temperature and frequency via the modulation of the conductivity of the inversion layer, *without* explicit reference to the density of states, except through the conductivity. When the Fermi level is in the localized portion of the density of states between the Landau levels (quantum Hall effect), the conductivity decreases rapidly and is difficult to measure; the capacitance signals, however, persist as the conductivity falls by many orders of magnitude. A new theoretical model of this resistive-capacitive, two-dimensional layer was developed which successfully accounts for the predominant features of the data and allows extraction of conductivity information from the capacitance measurements. Although previously the capacitance was thought to provide a mechanism for directly determining the density of states, this is shown not to be possible. Using the model to extract the conductivity, the temperature dependence of σ_{xx} was found to be activated, i.e., $\ln\sigma \sim 1/T$, in agreement with other measurements. No appreciable frequency dependence of σ_{xx} was found over a two-decade range of frequency.

I. INTRODUCTION

A substantial body of knowledge has been obtained over the last decade in the study of two-dimensional layers in semiconductors.[1] The density of states of an electron system determines many important behavior characteristics. Most studies of the density of states of two-dimensional systems are made via transport measurements, e.g., conductivity. The conductivity in these systems in a magnetic field, B, however, can fluctuate widely, and, in certain regions of theoretical and experimental interest, vanish (or nearly so) altogether. The early motivation for this work was based on the assumption that, since capacitance is a charge-sensitive measurement, it would be able to directly measure the density of states $D(E,B)$. Some early work in this area was carried out by Zemel and Kaplit[2] and by Voshchenkov and Zemel,[3] but new information and interest stimulated by the quantum Hall effect (QHE) has motivated this attempt to update and expand the capacitance technique that they pioneered. Our conclusion, based on a new understanding of the complications in the device, indicates that it is probably impossible to directly determine the density of states with capacitance. This work deals with the use of the capacitance technique together with a new way of interpreting the measurements which effectively amplifies the behavior of the conductivity in the important regions where it is difficult to measure directly.

Early theoretical studies[3] used combinations of lumped resistors and capacitors in an attempt to model the two-dimensional (2D) capacitance measurements. A later model by Stern[4] used a one-dimensional distributed system of resistors and capacitors. These discrete component models did not lend themselves to extraction of physically interesting quantities from the measurements. This paper describes a new, two-dimensional model based on a single physical parameter, the conductivity.[5]

The measured capacitance signals are shown to exhibit the form predicted, and deconvolution to obtain the conductivity is demonstrated. Of recent interest in the study of 2D systems is the notion of "localized states" of electrons. Information about these states is difficult to obtain since the conductivity drops to very low levels as more of the electrons become localized and, therefore, unable to conduct. The temperature and frequency dependence of the conductivity are derived from the capacitance data in the QHE region and are compared with current understanding of localization.

The capacitance model can be used to compare the rather complicated capacitance signals with the theoretical understanding of the 2D EG so that information might be inferred from the capacitance measurements. Of key importance is the relationship between capacitance and conductivity, since the conductivity reflects the underlying density of states. Although the density of states is not explicitly contained in the capacitance model, theoretical relationships between the conductivity and the density of states are possible. A calculation shows that even a simple example of such a relationship is able to accurately recreate most of the important features of the data.

A. Samples

The samples used throughout this work were silicon metal-oxide-semiconductor field-effect transistors (MOSFET's). A matrix of different Corbino disk geometries as well as a sample containing both a Corbino

 ©1985 The American Physical Society

TABLE I. Device characteristics.

Sample	d_{ox} (Å)	L (μm)	W (μm)	μ (cm^2/V sec)
Tektronix Corbino[a]	488	30	660	5430–6600
Bell Labs Corbino[b]	10 500	60	1200	2850
Bell Labs Hall bar	10 500	1000	200	2850

[a] Provided courtesy of Jeff Harrang and Tektronix, Inc.
[b] Provided courtesy of D. C. Tsui, then at AT&T Bell Laboratories.

disk and a Hall bar were available. Table I lists the characteristics of various samples used.

All the capacitance data were taken using the annular Corbino geometry. When a magnetic field is applied perpendicular to the plane of the Corbino sample the current moves in a logarithmic spiral path between the source and drain. Since symmetry prevents the establishment of a Hall electric field in the tangential direction, there is no contribution to the measured conductivity from nondiagonal terms in the conductivity tensor so that a direct measure of σ_{xx} is obtained. The Hall bar is a complementary configuration to the Corbino disk and was used to observe the quantum Hall effect for comparison with the capacitance data. Here the Hall electric field *is* established when a magnetic field is applied, and the current flows in a path that is complicated close to the source and drain ends. By using a constant channel current the resistivity tensor components ρ_{xx} and ρ_{xy}, measured at points away from the source and drain, are easily obtained. Note that a two-point conductivity measurement made between the source and drain contacts will yield a combination of σ_{xx} and σ_{xy} which is not easily deconvolved.[6] Because the combination of the two tensor components never gets small at high magnetic fields, the capacitance technique, which is sensitive to small *effective* conductivities, is not a useful tool for probing the bar geometry.

II. CAPACITANCE TECHNIQUE AND MODEL

A technique was developed capable of measuring extremely small capacitances (below 30 fF with a resolution of better than 0.1 fF) using measurement frequencies from 20 kHz to near the dc limit (<10 Hz). The capacitance method used in this study is to apply a dc bias and a superimposed ac modulating voltage to the gate, and measure at a channel contact (source or drain) the components of the induced current both in- and out-of-phase with the modulation voltage. That a phase-sensitive measurement of the current can provide a way of determining impedance parameters is most easily seen in the simple case of applying an ac voltage, V_0, to a series RC circuit. The complex current I is

$$I_+ = \frac{\omega^2 V_0 R C^2}{1+(\omega RC)^2} \text{ and } I_- = \frac{\omega V_0 C}{1+(\omega RC)^2}, \quad (1)$$

where I_+ and I_- refer to the real and imaginary components of the current. These correspond identically with the signals taken from the in-phase and out-of-phase lock-in amplifier outputs (measured with respect to the phase of the modulation voltage, V_0). Equation (1) can be inverted to obtain the values of R and C,

$$R = \frac{V_0 I_+}{I_+^2 + I_-^2} \text{ and } \frac{1}{C} = \frac{\omega V_0 I_-}{I_+^2 + I_-^2}. \quad (2)$$

Note that in the case where R is negligible, $I_- = \omega V_0 C$, the expected result for the ac current through a pure capacitor. This relationship also holds for the oxide capacitor, C_{ox}, formed by the gate of the MOSFET and the 2D EG, allowing calibration of the oxide capacitance.

The schematic of a typical capacitance-voltage measurement is shown in Fig. 1. Since most measurements reported are of capacitance as a function of V_g, the term "C-V" is used by analogy with the standard device characterization tool. When the gate voltage of a MOSFET is changed, the number of electrons in the inversion layer also changes, so a small ac voltage on the gate induces periodic fluctuations in the inversion-layer charge density. To effect these density changes charges must move in or out of the inversion layer via the channel contacts. At the low temperatures used in these experiments (1.3 K), charge-density changes by electron-hole recombination are

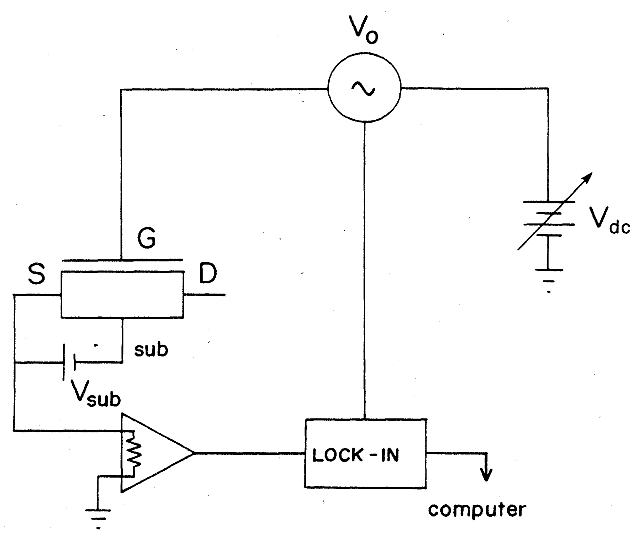

FIG. 1. The schematic arrangement of a capacitance measurement. The ac modulation, V_0, is superimposed on a slowly varying dc bias, V_{dc}, which is controlled by the computer. The current from the device is converted to a voltage by a current sensing preamplifier. The lock-in amplifier provides outputs both in-phase and out-of-phase with the modulation, corresponding to the real and imaginary components of the device current. The computer reads the lock-in output several hundred times and averages to improve the signal-to-noise ratio.

not possible, and if neither the source nor the drain is connected, no C-V signal is observed; the depletion-layer boundary is therefore shown to be frozen. Because all the measured current must flow through the channel, not only the oxide capacitance but also the channel resistance contribute to the measured impedance of the system. Initially one might suppose that this would pose no difficulty since, after threshold, the inversion layer is metallic. In the presense of a large magnetic field, however, the conductivity of the inversion layer undergoes extreme fluctuations, approaching zero in some circumstances, and this radical behavior will be reflected in any measurement of the device impedance. The fact that the conductivity of the device plays a part in the measurement means that this technique can be used to study electron transport. More importantly it means that early attempts to actually measure the density of states in a MOSFET *directly* with ac capacitance can never succeed. When the Fermi level is between Landau levels the simple $C = dQ/dV$ type of argument is obscured by the resistance of the channel becoming a strong (and unknown or model-dependent) function of the density of states. The best that can be accomplished is to extract information about the conductivity. In order to do this, however, one is required to develop a model for the capacitance behavior of the 2D EG.

A. Early device models

When the quantum limit of this system was first investigated,[3] the Si MOSFET was modeled using discrete components to represent the various conceptual parts of the system [see Fig. 2(a)]. The lumped circuit elements representation was initially developed to explain the *room-temperature* behavior of these devices. This model is insufficient to describe the behavior of the system when quantized at low temperatures. It is, however, useful as a visualization of the various components and represents the predominant conceptualization of the system until the present work. The model is based on the charge distribution which exists in MOSFET's in inversion, shown in Fig. 2(b).[7] The dominant component is the oxide capacitor, C_{ox}. At room temperature both the inversion layer and the depletion region change their charge density in response to changes in the gate voltage. The capacitor C_d represents the change in depletion charge (at the back edge of the depletion region) when more voltage is applied to the gate. The inversion layer at the Si-SiO_2 interface is modeled separately as a resistor, R_i, and a capacitor C_i. R_i is the resistance of the channel, and C_i represents the change in inversion-layer charge when the surface potential changes, dN/dV_s. This should, in principle, be related to the density of states, dN/dE_f. This early study did not include such a calculation, and no explicit extraction of $D(E)$ was published.

In 1974 Stern[4] extended the discrete-component model by taking the limit of a one-dimensional system of infinitesimal resistors and capacitors. The potential as a function of position in the discrete-component chain was determined, and the measured current was to be calculated. The circuit element, C_i, was again used and was related to the density of states via a variational calculation,

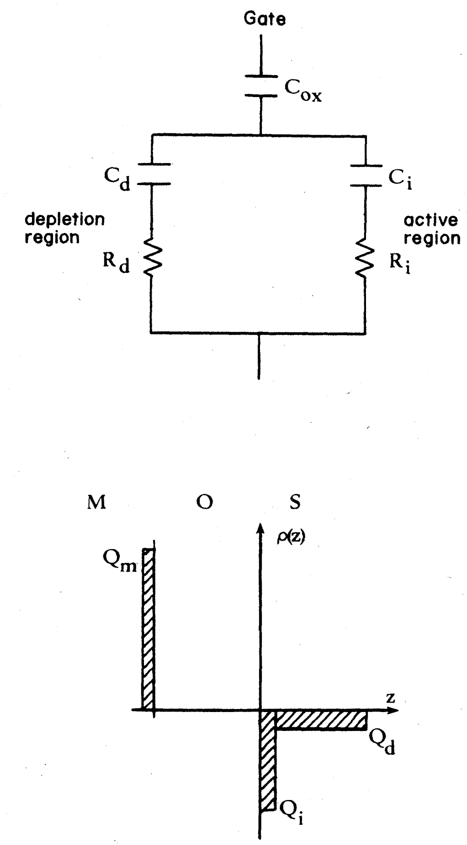

FIG. 2. (a) The model for the 2D EG used in Ref. 3. The arrangement of the components reflects the room-temperature model used by device engineers for MOSFET's. (b) The charge density as a function of z in a MOSFET. The positive charge on the gate metal, Q_m, is compensated by negative charge in both the inversion layer, Q_i, and the depletion region, Q_d. The depletion charge is the result of the acceptor states moving below the Fermi level because of the band bending and becoming ionized. At the temperatures used in this experiment, most of this charge is frozen out.

with the essential result $C_i \sim D(E)$ for small $D(E)$. The form predicted for the measured current was

$$I \propto \frac{\tan(a/2)}{a/2}, \tag{3}$$

where $a = (i\omega R_i C_i)^{1/2}$. A difficulty arises when attempting to use the data to extract the density of states. The resistance of the channel, R_i, always appears as a product with C_i. Because R_i becomes difficult to measure in the QHE regime, there is no explicit way to extract C_i from the capacitance data alone.

Recently[8] it has been suggested that in the quantum-Hall-effect regime (when the Fermi level is between the Landau levels), the Hall resistance, $h/e^2 = 25\,879\ \Omega$, could be used, thereby allowing the extraction of $D(E)$, but the complicated current flow paths in the bar geometry device used and mixing of the tensor components of the conductivity in that geometry make the association of R_H with the distributed resistance of the one-dimensional Stern model questionable.

B. Resistive plate model

In this work a different approach was taken to interpret the C-V behavior of the 2D EG. Rather than trying to extract the density of states directly, the *conductivity* can be obtained. The conductivity is of importance in verifying models of electron behavior in crystals as well as features of the density of states. A model of the C-V current in the device from which information about the conductivity can be extracted is required. Earlier models treat the system as one dimensional when, in fact, the material properties are determined by the two-dimensional nature of the system. The system is, therefore, treated as a two-dimensional annular capacitor with one metallic and one resistive plate with conductivity σ_{xx}. Because of the low temperature the depletion capacitance, C_d, can be initially neglected, as experimentally verified above.

Assume linear response:

$$\mathbf{J} = \overleftrightarrow{\sigma}\cdot\mathbf{E} = -\overleftrightarrow{\sigma}\cdot\nabla V, \tag{4}$$

where

$$\overleftrightarrow{\sigma} = \begin{bmatrix} \sigma_{xx} & -\sigma_{xy} \\ \sigma_{xy} & \sigma_{xx} \end{bmatrix},$$

and $V(r,t)$ is surface potential at position r in the channel (see Fig. 3). Because of the circular symmetry no physically relevant quantity can depend on theta. This gives

$$J_r(r) = -\sigma_{xx}\frac{dV(r)}{dr}. \tag{5}$$

The continuity equation,

$$\nabla\cdot\mathbf{J}(r,t) = -\frac{\partial Q(r,t)}{\partial t}, \tag{6}$$

can be written

$$\frac{dJ_r(r)}{dr} = -\frac{dQ}{dV_g}\frac{\partial V_g(r,t)}{\partial t}. \tag{7}$$

It should be noted that the second term of the gradient in Eq. (6), $(1/r)\partial J_\theta/\partial\theta$, which arises in the cylindrical coordinate system, is zero by symmetry. Only the radial component of the current is relevant, and the two-dimensional nature of the calculation is less evident. It is fundamental to the Corbino geometry that σ_{xy} plays no part in determining the source-drain current.

The "effective" gate voltage at any point in the channel plus the voltage drop along the channel must equal the applied voltage (see Fig. 3),

$$V_g(r,t) + V(r,t) = V_{\mathrm{dc}} + V_0 e^{-i\omega t}, \tag{8}$$

so that

$$\frac{\partial V_g(r,t)}{\partial t} = -i\omega[V_0 - V(r)]e^{-i\omega t}. \tag{9}$$

Since all quantities have a common factor, $e^{-i\omega t}$, it will be dropped from subsequent equations. Note, however, that the spatial functions are *complex*. Substituting Eq. (9) into Eq. (7) yields

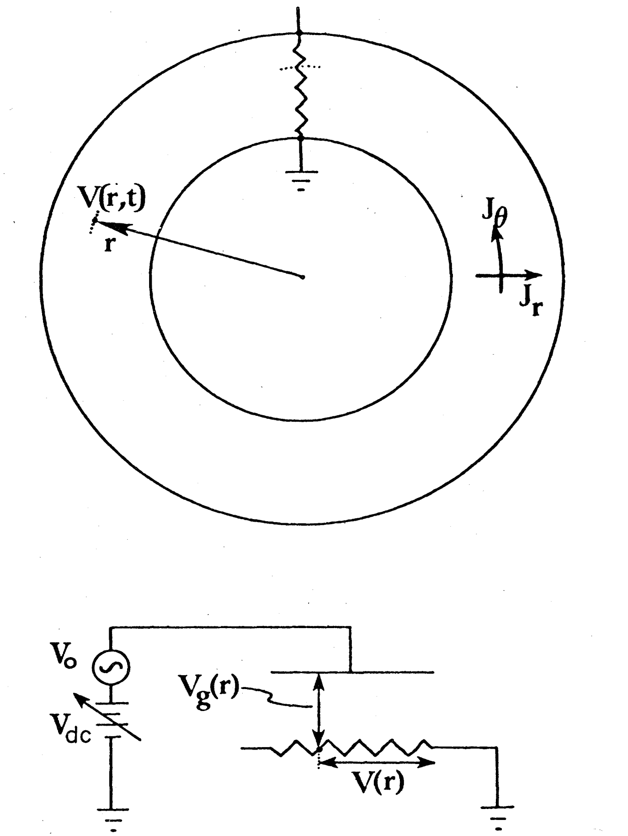

FIG. 3. The resistive plate model of the 2D EG developed in this work. $V(r,t)$ is the surface potential. The current in the resistive system is shown to depend only on the conductivity of the inversion layer.

$$\frac{dJ_r(r)}{dr} = i\omega C_{\mathrm{ox}}[V_0 - V(r)], \tag{10}$$

where dQ/dV_g has been replaced by C_{ox} (with dimensions of $\mathrm{F/cm^{-2}}$). In previous works the concept of "inversion-layer capacitance" was introduced instead. V_g was no longer considered proportional to N, and the data were explained as effects of C_i (despite the difficulty introduced by R_i). However, here dN/dV_g is assumed always constant $[=(1/e)C_{\mathrm{ox}}]$, and when the Fermi level is between Landau levels, *localized* states are being filled as the dc bias is being swept. The features of the data are due to the conductivity changing, *not* an explicit effect of $D(E)$. Given sufficient time to respond, a change in the gate voltage, ΔV_g, will *always* induce a change in the inversion-layer charge density equal to $(dN/dV_g)\Delta V_g$.

Taking another derivative with respect to r in Eq. (10) and using Eq. (5) produces the following differential equation for the current density:

$$\frac{d^2J_r(r)}{dr^2} + \alpha^2 J(r) = 0, \tag{11}$$

where the complex quantity $\boldsymbol{\alpha}$ is given by

$$\alpha = \left[\frac{i\omega C_{ox} L^2}{\sigma_{xx}} \right]^{1/2} , \tag{12}$$

and L is the length of the channel. Using the appropriate boundary conditions one obtains the predicted form of the C-V current,

$$I_{C\text{-}V} = I_{C\text{-}V0} \frac{\tanh(\alpha)}{\alpha} , \tag{13}$$

where $I_{C\text{-}V0}$ is the current that flows in the metallic case, i.e., when σ_{xx} is very large. [Note that because of the relationship between tanh and tan for imaginary arguments, i.e., $\tanh(ix) = i\tan(x)$, the relationship developed by Stern, Eq. (3), predicts the same *form* for the current as Eq. (13). This is a universal form for the current in a distributed resistive-capacitive system.]

Equation (13) indicates that the measured current should be parametrized by the single quantity, α. Figure 4 shows the form of I_+ and I_- as a function of α ($\alpha = |\alpha|$). This curve contains all the information about the C-V current, and will henceforth be referred to simply as "$\tanh(\alpha)/\alpha$." Several features are noteworthy for later comparison with the data.

(1) When the conductivity is large (small α) the imaginary component of the current is near one and the real component is small. This is the region where the device behaves essentially like a two-plate capacitor; the impedance approaches $1/i\omega C_{ox}$.

(2) As the conductivity falls and α rises, the real and imaginary parts of the current approach each other. As the two curves near each other, the real part peaks and then the curves meet. The peak in the real part occurs when

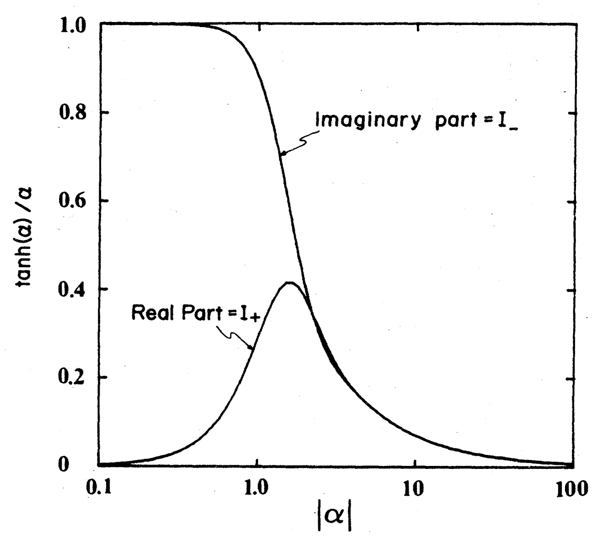

FIG. 4. The theoretical form of the capacitance current which predicts how the real and imaginary parts of the measured current should depend on the frequency and conductivity. Using Eq. (12) the measured I_+ and I_- currents can be inverted to determine the conductivity at a given frequency. Note that since $\alpha^2 \sim 1/\sigma$, this curve covers six orders of magnitude of conductivity.

$$\frac{I_-}{I_+} = \frac{0.620}{0.415} = 1.49 \;\; (\alpha = 1.512),$$

and the two curves meet when

$$I_- = I_+ = 0.345 \;\; (\alpha = 2.263).$$

These conditions will allow correct alignment of the data and model. This regime corresponds to the resistive and capacitive components of the impedance being within about two orders of magnitude of each other at the measurement frequency.

(3) When the conductivity becomes very small, the real part follows the imaginary part downward toward zero. In this regime the conductivity has fallen to such an extent that the resistive component of the impedance dominates the signals. The system behaves like a resistive transmission line where the output is phase shifted 45° with respect to the input.

In summary, the resistive plate model differs from those previously used to describe the 2D EG in a MOSFET. As indicated above, models which treat the inversion layer independently require two quantities, R_i and C_i, to determine the density of states explicitly, and these are not clearly defined from an experimental or theoretical point of view. Equation (13), however, even though it is similar to the current relationships determined by Stern, is based on only one well-defined physical quantity, the conductivity. Although the density of states is not explicitly available, σ_{xx} itself is important for understanding these systems. In the next section the measured C-V signals are presented, and are seen to reflect the $\tanh(\alpha)/\alpha$ behavior developed here. In Sec. IV the relationship represented by Eq. (13) is used with simple assumptions about the conductivity and its dependence upon the density of states to predict the C-V current.

III. MEASUREMENTS

In this section general aspects of the capacitance data will be discussed, and a comparison of C-V with conductivity will show how the capacitance can augment the conductivity measurements. Unless otherwise specified, all measurements were made at a temperature of 1.3 K and a frequency of 1000 Hz. Applied magnetic fields were always perpendicular to the plane of the 2D EG.

A. General features of capacitance data

Figure 5 shows the capacitance of a MOSFET with no applied magnetic field. Several features common to all C-V measurements should be noted.

(1) Capacitance data *always* consists of two curves which are the in-phase and out-of-phase components of the lock-in output. As previously discussed these correspond to the real and imaginary components of the calculations. For all the data presented the real (in-phase) component will be labeled I_+, and the imaginary (out-of-phase) component will be labeled I_-.

(2) Over most of the gate voltage sweep both parts of the signal are constant and the imaginary part is much

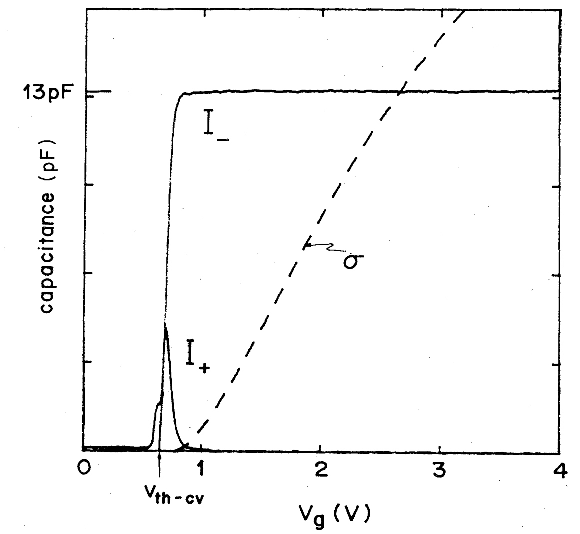

FIG. 5. The $B=0$ T capacitance. The real part I_+ and the imaginary part I_- of the measured current as a function of V_g. The threshold, V_{th}, is much more sharply defined by the capacitance than the conductivity, which is shown as the dashed curve. After threshold I_- reaches a plateau which is effectively the oxide capacitance, ≈ 13 pF.

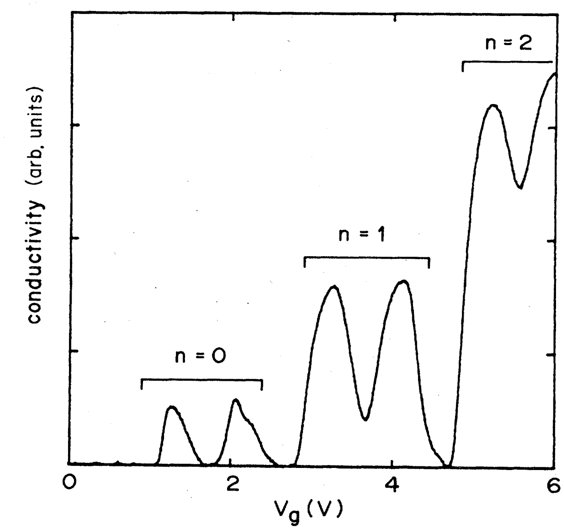

FIG. 6. The $B=9$ T conductivity. When a large magnetic field is applied the density of states is quantized and this is reflected in the conductivity. The Landau levels are labeled (n). When σ goes to zero over a finite span of V_g, localization is occurring (the quantum-Hall-effect region).

larger than the real part. This is the general signature of metallic conductivity in the 2D EG. The device is essentially a two-plate capacitor with impedance $1/i\omega C_{ox}$ and the current associated with that impedance will be nearly aligned with the imaginary axis. This corresponds to the region of small α in the resistive plate model.

(3) The turn-on of the capacitance is rather sharp with I_- rising rapidly to its plateau level and I_+ having a peak before falling to a low value. This is a characteristic relationship between the real and imaginary parts of the model.

Also shown in Fig. 5 is the conductivity (dashed line). Here is an example that the C-V can provide information that is not easily obtained from the conductivity. The threshold voltage, V_{th}, is more sharply defined in the capacitance data and is clearly lower than would be estimated from conductivity measurements.[9] Data from many different samples indicates that the threshold measured by conductivity could differ by several volts from that measured by C-V.

We show in Fig. 6 the conventional conductivity σ_{xx} with $B = 9$ T. This data, measured on the *same* sample as the capacitance data to be presented, displays the familiar conductivity features of the QHE. The conductivity has peaks when the Fermi level is in a region of high density of states and goes to zero when the Fermi level is a region of low density of states. Since the energy gap between levels is only a few meV, a cusp would normally be expected between the peaks in the conductivity (actually a narrow gap of a few mV in gate voltage). The wider region of gate voltage over which σ_{xx} is zero is attributed to the filling of localized states which do not contribute to the conductivity, and is the region where the Hall resistance attains a quantized plateau (the quantum Hall effect). When the density falls below some value, the conductivity exhibits a "mobility edge." Although there is no conduction *across* the channel, localized states are being filled, so a finite region of gate voltage is traversed.

Figure 7 shows the capacitance with a 9-T magnetic field applied. The striking feature is the presence of structure between the levels—precisely where the conductivity of Fig. 6 was small. Several features are of note.

(1) The model developed in Sec. II B is in general agree-

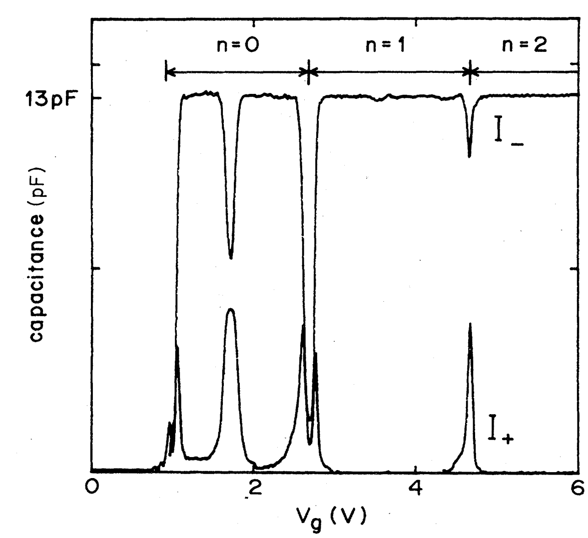

FIG. 7. The $B=9$ T capacitance. The capacitance current is modified from its $B=0$ value in precisely the regions where σ is small in Fig. 6. The behavior of the C-V current also reflects the form of Eq. (13). The double hump structure in I_+ at the $n=0 \rightarrow n=1$ Landau-level gap is the signature of moving over the peak in the real part of $\tanh(\alpha)/\alpha$ in Fig. 4 and then back again.

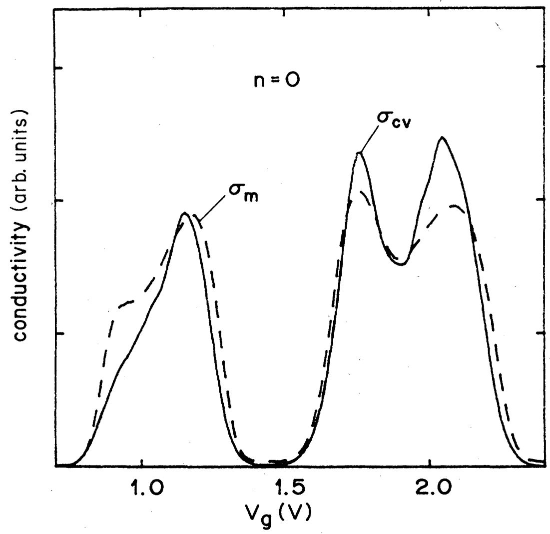

FIG. 8. Detailed comparison of measured and derived conductivities. The measured conductivity, σ_m (dashed curve), and the measured conductivity, $\sigma_{C\text{-}V}$ (solid curve), in the first Landau level.

ment. The real part of the signal is near zero when the imaginary part is at its plateau, and rises when the imaginary part falls.

(2) The double peak structure in I_+ results from the decreasing conductivity between Landau levels making α large [Eq. (12)], and thereby moving the measurement over the peak in the real part of the $\tanh(\alpha)/\alpha$ curve (Fig. 4). As σ increases upon exiting the Landau gap, the process is mirrored.

(3) As seen in the $B=0$ data, when the conductivity is large, the capacitance does not contain much information.

(4) The most important feature is the existence of accurately measurable signals in the regions of gate voltage where the conductivity is small. The conductivity and density of states can be extracted in this region where localization is occurring. The experimental variable's temperature and frequency will be investigated with regard to their effect on the 2D EG at values of gate voltage corresponding to a wide range of density and conductivity behavior.

Figure 8 shows the first Landau level of the measured conductivity, σ_m (dashed line), and the conductivity derived from capacitance, $\sigma_{C\text{-}V}$ (solid curve). The $\sigma_{C\text{-}V}$ was obtained from the measured C-V of Fig. 7 by numerically inverting $\tanh(\alpha)/\alpha$ to yield α, and then calculating α from Eq. (12). Although the general form of the measured conductivity is remarkably well reproduced, the vertical scale of $\sigma_{C\text{-}V}$ is systematically underdetermined by a factor of order 100 compared to the data. This is presently not understood, although a possible explanation is discussed at the end of Sec. IV.

B. Temperature

The conductivity is sensitive to temperature when the 2D EG is localized. In this section the temperature behavior of the capacitance will be investigated at points where localization is expected to occur and the dependence of the conductivity on temperature will be extracted.

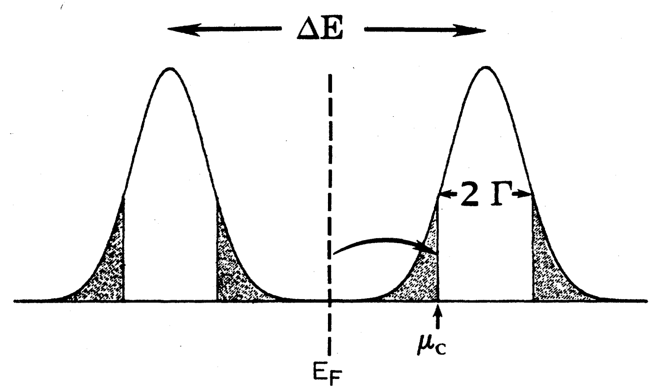

FIG. 9. Hopping conductivity. When the Fermi level is below the mobility edge, electrons are promoted via phonon assistance to the mobility edge in order to conduct.

Hopping (or activated) conductivity is expected for Anderson localization in the 2D EG of a Si MOSFET.[10,11] This type of system was shown by Mott to have a "mobility edge" below which the conductivity quickly vanished; these mobility edges are at the sides of bands where the density of states is small.[12] If the Fermi level is in the gap between two Landau levels, conductivity must be phonon

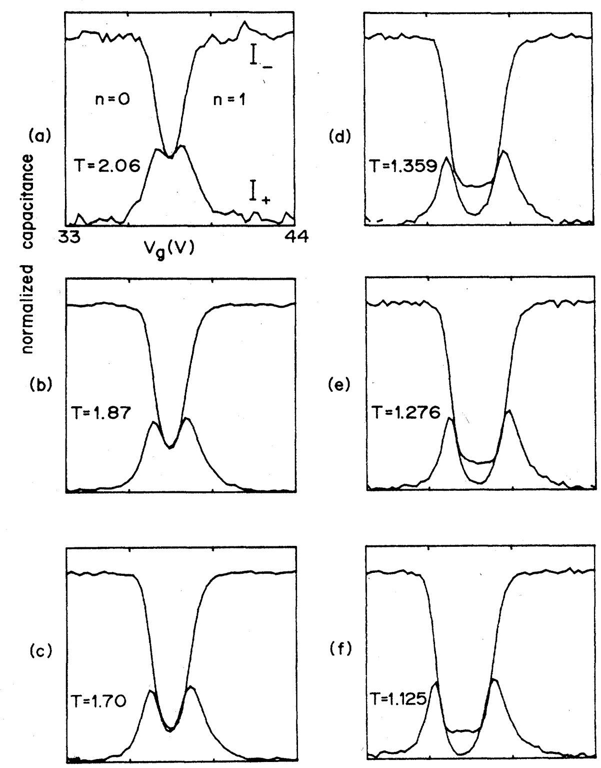

FIG. 10. Temperature dependence of the capacitance. The capacitance measured at the $n=0 \rightarrow n=1$ Landau gap on the Bell Corbino sample at six different temperatures. (a) 2.06 K, (b) 1.87 K, (c) 1.70 K, (d) 1.359 K, (e) 1.276 K, and (f) 1.125 K. The diminishing of the C-V structure with increased temperature is due to the increase of σ which results from the disappearance of localization.

assisted (see Fig. 9). Since the conductivity depends on the number of electrons which can be thermally promoted to available final states, when E_f is in the center of the gap,

$$\sigma = \sigma_{\min} e^{-(\Delta E - 2\Gamma)/2k_B T}, \tag{14}$$

where ΔE and Γ are the spacing and width of the Landau levels, respectively. This provides a mechanism for determining the effective level width as well as verifying the form of the localization.

Figure 10 shows the real and imaginary parts of the capacitance as a function of V_g around the $n=0 \rightarrow n=1$ Landau gap for six different temperatures measured on the Bell Corbino sample. The increasing strength of the capacitance structure reflects the decrease in σ with T. Figure 11 shows the capacitance (normalized to the oxide level) plotted as a function of $1/T$ for a Tektronix Corbino sample with V_g *fixed* at the center of the $n=0 \rightarrow n=1$ Landau gap. The data clearly follows the form of $\tanh(\alpha)/\alpha$, so that extraction of conductivity information is possible using Eq. (12). Figure 12 shows the least-squares fit of the data to Eq. (14). The position of the mobility edge with respect to the band center is Γ in Fig. 9. The analysis of Fig. 12 gives $\Gamma = 2.013$ meV, giving a localized region of ~ 1.4 meV in the density of states between the first and second Landau levels. These results confirm activated conductivity and demonstrate the ability of capacitance to yield important information about the 2D EG.

Measurements[13,14] indicate that in Si, where surface roughness is the predominant scattering mechanism for the electrons, the classically measured lifetime (from low-B-field mobility) and the quantum lifetime (width of the Landau levels) should be about the same. If Γ derived above is converted to an effective broadening,[15] it corresponds to a low-field mobility of ≈ 5230 cm^2/V sec, compared with the measured low-field mobility of 5400 cm^2/V sec. The mobility edge linewidth is, thus, close in value to the impurity broadened linewidth.

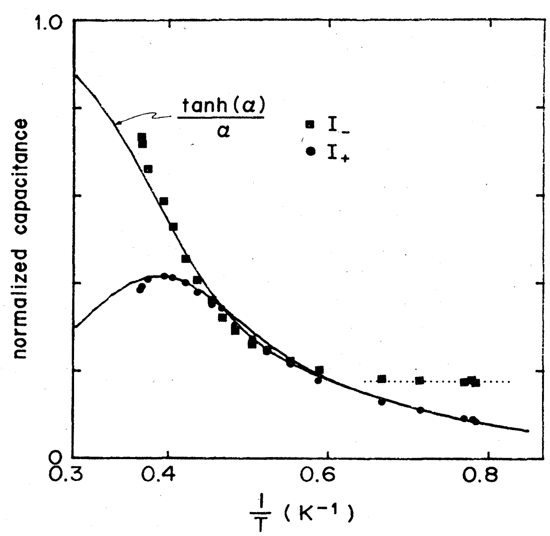

FIG. 11. The temperature dependence of the C-V at the bottom of the $n=0 \rightarrow n=1$ Landau gap. The solid lines are a least-squares fit of $\tanh(\alpha)/\alpha$ to the data, and agree well except for the capacitance signal, I_-, at the lowest T. The systematic divergence of I_- there is attributed to stray capacitances, e.g., depletion capacitance. Because this interference is predominantly in the 90° quadrature of the signal, the conductance, I_+, is not effected.

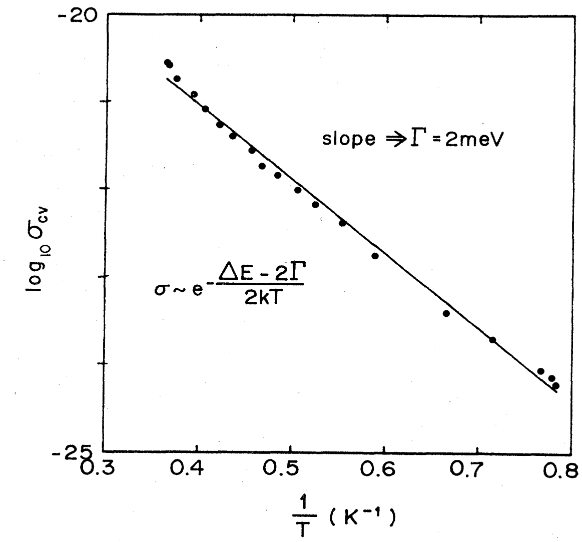

FIG. 12. The extracted conductivity plotted against T^{-1}. The slope of the line gives the activation energy which is interpreted as an effective broadening of the Landau levels.

C. Frequency

Another rather different view of localization pictures a surface potential containing hills and valleys where pools of electrons can become energetically trapped. As more electrons are introduced the connected regions grow in size until a filling level is reached where there exists a connected path throughout the potential and conduction can begin. A useful concept is that of a "localization length," i.e., the size of the region in which an electron is localized.[16] If the localized electrons are being driven by an ac source, at low frequencies they will continue to appear localized since there is sufficient time per cycle to drift to the edge of the confining potential. At some frequency, however, the drift distance will become less than the localization length,

$$\frac{v_H}{f} \lesssim d_{\mathrm{loc}}, \tag{15}$$

and the localization should be less evident.

Figure 13 shows how the C-V signal varies across the first Landau level as a function of frequency for the Tektronix Corbino sample. As the density of free charge decreases (when the Fermi level is in the Landau or spin gap), the capacitance reflects the marked decrease in the conductivity as expected. As the frequency is decreased at a particular V_g, the capacitance structure is diminished. The parameter α is an explicit function of frequency, however, and the behavior in Fig. 13 can be explained by this dependence on f alone, and no functional systematic

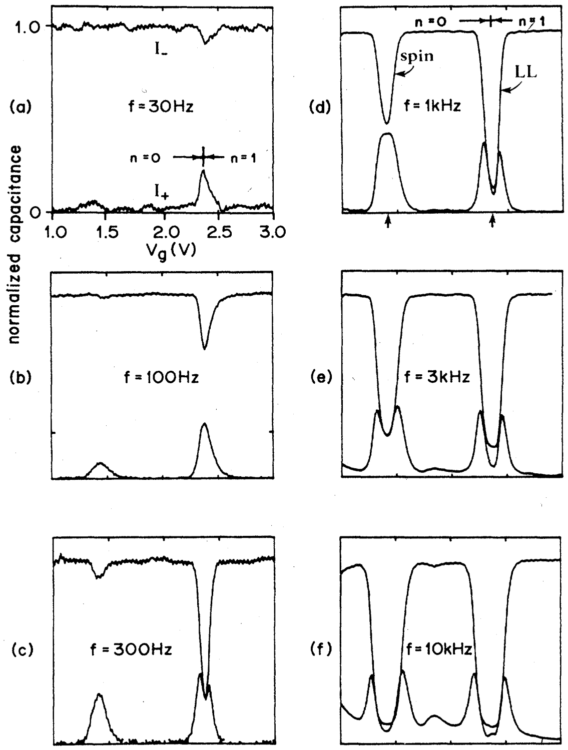

FIG. 13. Frequency dependence of the capacitance. The capacitance measured on a portion of the first Landau level of the Tektronix Corbino sample at six different frequencies. (a) 30 Hz, (b) 100 Hz, (c) 300 Hz, (d) 1 kHz, (e) 3 kHz, and (f) 10 kHz. The change in the C-V structure reflects the dependence of $\tanh(\alpha)/\alpha$ on frequency, and not any dependence of σ on f. When the frequency was below about 9 Hz the C-V structure was not observed at all. The arrows indicate where the analysis described in the text occurs.

dependence of σ on f is necessary. The explicit frequency dependence of α is suppressed by the following procedure:

(1) Choose a value of gate voltage at which to deduce σ. For this example the two QHE regions, $V_g = 1.4$ V (spin gap), and $V_g = 2.35$ V (Landau gap), were used. These points are indicated by arrows in Fig. 13(d).

(2) At each frequency find the value of α which best fits the real and imaginary parts of the data on the $\tanh(\alpha)/\alpha$ curve.

(3) Since $\alpha^2 \propto f/\sigma$, taking the logarithm of both sides yields

$$\ln\alpha = \tfrac{1}{2}\ln f + \tfrac{1}{2}\ln\frac{K}{\sigma}\,. \tag{16}$$

A least-squares fit of the α values obtained in step (2) using the form of Eq. (16) is shown in Fig. 14. The top curve is the Landau gap data, and the bottom curve is the spin gap data. The fit to a straight line indicates that σ has no significant frequency dependence at these frequencies. The y intercepts of the two lines allow the determination of the conductivity ratio between the spin gap and the Landau gap,

$$\frac{\sigma_s}{\sigma_L} = 10.17\,.$$

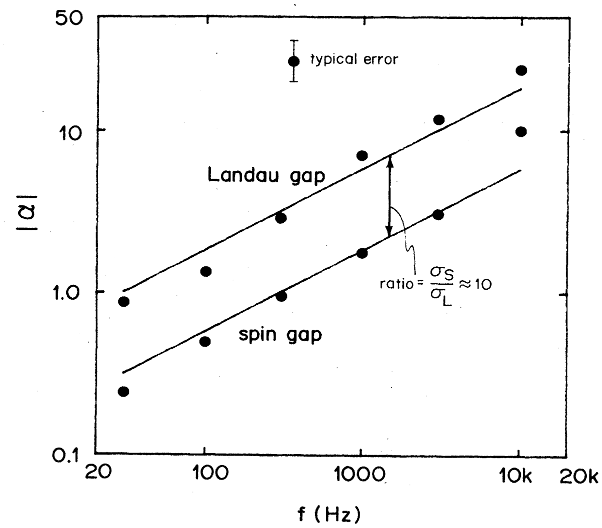

FIG. 14. Least-squares straight-line fit of relationship between α and f to the frequency data indicating that the conductivity has no appreciable frequency dependence. The top curve is from the $n=0 \rightarrow n=1$ Landau gap, and the bottom curve is from the $n=0$ spin gap.

This information, which is difficult to obtain from direct conductivity measurements (see Fig. 6), indicates that the localization in the region between Landau levels is much stronger than that in the region between the two spin states which agrees with a model of the density of states to be developed in Sec. IV.

It is important to note another aspect of the frequency data. As the frequency is decreased, the capacitance structure is diminished. If the frequency is made low enough, the structure disappears altogether. This occurred at about 9 Hz in this sample. This is definitive evidence that the C-V in a MOSFET does not provide information about the density of states even if the frequency is made very low, as thought by earlier researchers.[3] The fluctuations in the capacitance are completely explainable by the effect of the conductivity in a resistive-capacitive system.

D. Fraction of localized states

Figure 15 shows the resistivity tensor components, and the C-V signals of a MOSFET measured on the same chip (Bell Hall bar and Corbino disk, respectively). The measurement was made near the $n=0 \rightarrow n=1$ Landau gap. The Hall resistivity, ρ_{xy}, shows the quantum-Hall-effect plateaus, and the measured Hall resistance of 6436 ± 1 Ω was $h/4e^2$ within our experimental accuracy.

Because the increase in the 2D EG density is proportional to V_g, it is common to consider the ratio

$$f_{\mathrm{loc}} = \frac{\Delta V_{\mathrm{Hall}}}{\Delta V_{g-\mathrm{LL}}} \tag{17}$$

as the fraction of localized states in the 2D EG.[17] ΔV_{Hall} is the width in gate voltage of the QHE plateau and $\Delta V_{g-\mathrm{LL}}$ is the spacing in gate voltage of the Landau lev-

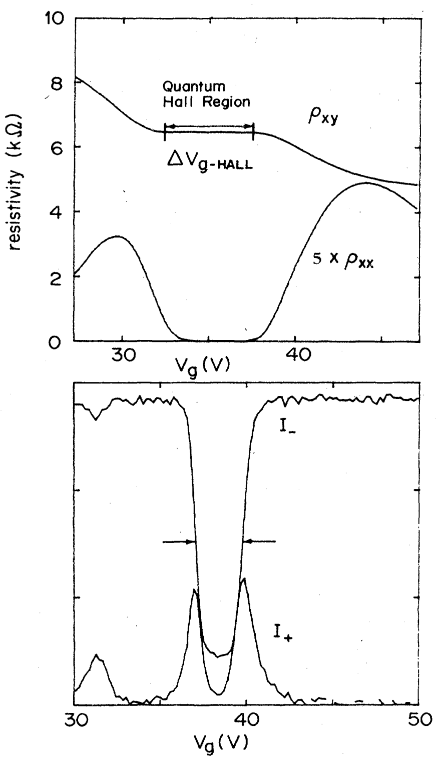

FIG. 15. The quantum Hall effect. (a) The resistivity tensor components measured on the Bell Hall bar near the $n=0 \rightarrow n=1$ Landau gap. ρ_{xx} is multiplied by 5. The value of ρ_{xy} at the plateau is with 0.3% of the expected value of $h/4e^2$. (b) The capacitance of the Bell Corbino sample measured at the same place as the resistivity. The capacitance provides a sharp indication of when ρ_{xx} (or equivalently, σ_{xx}) falls indicating that the QHE is occurring.

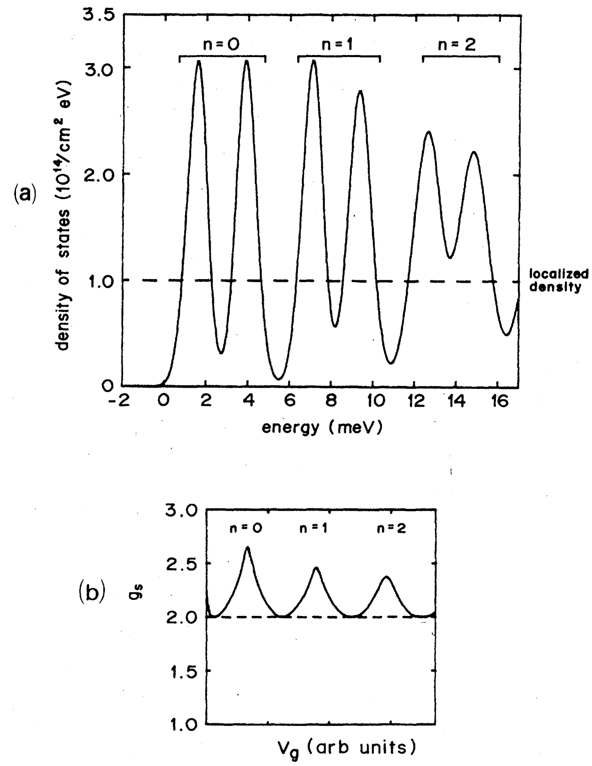

FIG. 16. (a) The density of states used to generate theoretical C-V. To properly account for the width in V_g of the measured capacitance structure in the QHE region, a background density (shown dashed) was required. (b) The g factor that was required to obtain agreement with the data.

els. The ρ_{xy} data of Fig. 15(a) indicates that approximately 13% of the electrons are localized. However, f_{loc} determined this way depends upon the precision and flatness of the plateaus, and the size of ΔV_{Hall} depends upon how close to zero σ_{xx} is.[18] The C-V data shows that unless very severe constraints are placed on the "flatness" condition of σ_{xy}, the actual region over which the conductivity is dominated by the QHE is overestimated.

IV. CALCULATION OF THE QUANTIZED CAPACITANCE

In Sec. II a model of the inversion layer was developed which predicted the form of the capacitance current given the channel conductivity. This section will use some of the details of the behavior of a quantized 2D EG to generate theoretical corroboration for the rather complicated behavior of the capacitance seen in the previous section.

For this illustrative calculation σ_{xx} will be assumed to depend on the density of states in a particularly simple but physically meaningful way,[19] namely,

$$\sigma \propto D^2(E_f) . \tag{18}$$

There are two factors which dominate the description of the quantized density of states: (1) the overall form as a function of energy and (2) the broadening of the various components as a function of Landau-level index. For the samples used in this study the valley splitting is not very strong, and in the following will be ignored.

The most comprehensive theory of transport in the 2D EG (Ref. 15) predicts an elliptical form for the Landau levels. In this calculation a Gaussian form is used because it conveniently provides the more physical tapering of $D(E)$ at the band edge.

To introduce spin into the density of states naively requires only the determination of the spin splitting, $\Delta E_s = g_s \mu_B B$, where g_s is the Lande g factor, and μ_B is the Bohr magneton. The g factor usually has a value of 2, and with $B=9$ T this gives $\Delta E_s = 1.04$ meV (the Landau level spacing is 5.48 meV). In these 2D systems, however, the g factor is not constant at a value of 2, but oscillates due to exchange effects depending upon the position of the Fermi level.[20] There are theoretical calculations of this effect,[21] and here the form of the enhancement was approximated and scaled as necessary to give best agreement with the data.

The overall broadening as a function of gate voltage, and therefore Landau-level index, can be measured by the low-field mobility. Ando has calculated[15] the relationship between the low-B and high-B lifetimes as

$$\Gamma^2 = \frac{2}{\pi} \hbar\omega_c \frac{\hbar}{\tau_c} . \tag{19}$$

This was used to extract from low-B mobility data the overall form of the broadening of the Landau levels.

Figure 16(a) shows the density of states used. The amount of overlap between neighboring levels reflects the broadening, and increases in the higher Landau levels where the broadening is greater. Figure 16(b) shows the g factor which was used. The enhancement decreases with increasing V_g since the increasing broadening reduces the difference in population between adjacent spin levels. The conductivity was derived from this density of states using Eq. (18). In order to represent the effect of localized states, a constant background [shown dotted in Fig. 16(a)] was added to the density of states, and this was integrated to obtain $N \propto V_g$. This background was *not* included in the calculation of σ. The effect of this is to create a region of gate voltage over which the density is increasing, but the conductivity is low. This models the essential features of the density of states which lead to the quantum Hall effect. This calculated conductivity was used with the $\tanh(\alpha)/\alpha$ relationship to generate the predicted C-V curves shown in Fig. 17(a). Typical measured C-V data is shown in Fig. 17(b). The $\tanh(\alpha)/\alpha$ behavior is clearly seen in the region when the density of states is low (between the Landau levels). The conductivity used in Eq. (12) to generate Fig. 17(a) was scaled up by a factor of 10. This disagreement in the magnitude of conductivity is probably linked to a similar scale factor which occurs when inverting capacitance to obtain $\sigma_{C\text{-}V}$ in Fig. 8; both are discussed in the next section. The excellent overall agreement of this calculated capacitance to the highly structured C-V data is solid evidence that the basic interpretations made in the resistive plate model are valid, and provides additional evidence that the present picture of the 2D EG is accurate.

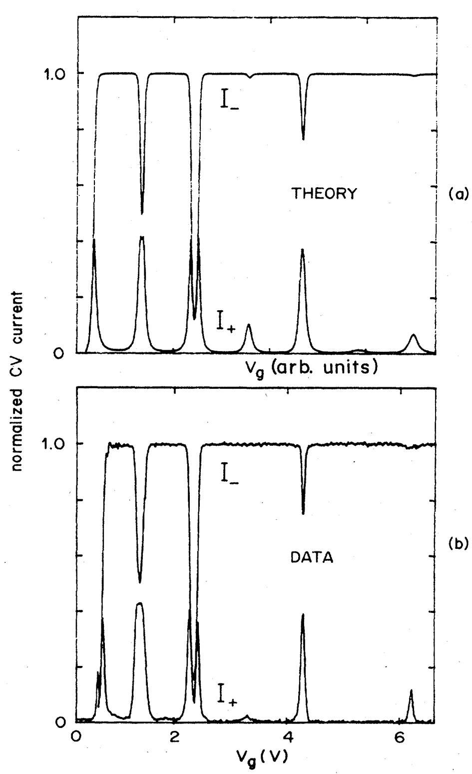

FIG. 17. Results of the calculation of the capacitance versus gate voltage. (a) The predicted form for the current as a function of V_g. (b) The measured C-V data. The agreement between the theory and the data is remarkable, and demonstrates that the resistive plate model assumed for the 2D EG is reasonable.

A. Circulating current

The disagreement between the absolute magnitude of the measured and derived conductivities is presently being investigated. Although not fully understood at this time, a likely cause for this discrepancy is the omission in the model of the induced EMF caused by the current, J_θ, which circulates around the Corbino disk (see Fig. 3).[22] The capacitance measurements were typically made with the outside annular contact floating.[23] Because of this, a Hall potential can be established at right angles to J_θ, which will *oppose* the potential induced by the flow of the radial current, J_r, through the resistive 2D layer. This will self-consistently reduce J_r, and, since the resultant potential is less than expected, cause an underestimation of the conductivity.

One might introduce this effect into the resistive plate formalism, through the following modification to Eq. (5):

$$J_r(r) = -\sigma_{xx}\left[\frac{dV_R}{dr} + \frac{dV_H}{dr}\right], \tag{20}$$

where V_R is the resistive potential, and V_H is the induced potential. Since an induced EMF would be proportional to $J_\theta = J_r\,\sigma_{xy}/\sigma_{xx}$, a second parameter is introduced into the model, namely the Hall conductivity, σ_{xy}. Because σ_{xy} is constant over the range of gate voltage relevant to capacitance measurements in the QHE region (see Fig. 15), its effect might be accounted for if the rather complicated differential equation derived from Eqs. (20) and (10) can be solved. This effort is currently under way. The constant level of σ_{xy} in the QHE region would also explain why the *form* of $\sigma_{C\text{-}V}$ agrees while its absolute magnitude does not.

If this explanation is borne out, it might provide direct evidence concerning the presence and magnitude of the dissipation-free, circulating Hall current.[24]

V. CONCLUSIONS

The capacitance technique developed here reflects the complexity which characterizes the 2D MOSFET system at low temperatures under magnetic quantization. The measurements made demonstrate that the capacitance can provide relevant physical information about the 2D EG. A new model was developed for the two-dimensional resistive system and successfully applied to measured data to extract meaningful information about the 2D EG. By treating the 2D EG as a resistive plate capacitor, the conductivity was the only physical parameter necessary for interpretation of the data. The model predicts a specific relationship for the real and imaginary parts of the measured current, $\tanh(\alpha)/\alpha$, where $\alpha = (i\omega C_{ox}L^2/\sigma_{xx})^{1/2}$. Although this form is similar to that developed by previous investigators, the relationship of the experiment and the theory is a new one, not the equivalent circuit model used previously. The advantage of capacitance is seen to be its ability to expose details of the behavior of the conductivity when the conductivity is very small. This is especially important in regions where the 2D EG is undergoing localization, since the conductivity is typically difficult to measure in these regions.

To investigate the capability of the capacitance to provide information about the conductivity when the 2D EG is localized, both the temperature and the frequency dependence of the capacitance were measured in the quantum-Hall-effect regime. When the conductivity was extracted from the capacitance data, the temperature dependence was found to be of the form expected for simple localization, i.e., $\ln\sigma \sim 1/T$. This corresponds to activated conductivity, where the electrons in the localized states between the Landau levels are promoted by low-energy phonons to the nearest mobility edge, the position of which is found to be far from the center of the band.

Using capacitance measurements to deduce the conductivity as a function of frequency from 10 Hz—20 kHz, no systematic frequency dependence was found.

Finally, to demonstrate how the capacitance-determined conductivity could aid theoretical studies the 2D EG, a calculation of the predicted form of the C-V data, was made. A form for the density of states consistent with present understanding of the 2D EG was used to generate predicted capacitance versus gate voltage relationships which agree well with the highly structured data. The calculation demonstrated that both g-factor enhancement and localized states are important in reproducing the form of the data, and provides confidence in the interpretations made about the capacitance measurement.

ACKNOWLEDGMENTS

The authors are grateful to Frank Stern for information on his early work in this area and for critical discussions of our experiment. One of us (R.J.H.) would like to thank Phil Stiles, Frank Fang, and Dan Tsui for useful discussions. Dave Cohen and Roger Haydock provided helpful input on various experimental and theoretical details, respectively. This work was supported in part by National Science Foundation Grant No. DMR 81-19550 and by the Tektronix Foundation.

[1]T. Ando, A. B. Fowler, and F. Stern, Rev. Mod. Phys. **54**, 437 (1982).
[2]J. N. Zemel and M. Kaplit, Surf. Sci. **13**, 17 (1969).
[3]A. M. Voshchenkov and J. N. Zemel, Phys. Rev. B **9**, 4410 (1974).
[4]F. Stern, IBM Internal Report, 1972 (unpublished).
[5]R. K. Goodall, R. J. Higgins, and J. P. Harrang, Bull. Am. Phys. Soc. **28**, 322 (1983).
[6]S. Kawaji, Surf. Sci. **73**, 46 (1978).
[7]S. M. Sze, *Physics of Semiconductor Devices* (Wiley, New York, 1969).
[8]L. C. Zhao and P. J. Stiles, Bull. Am. Phys. Soc. **28**, 323 (1983).
[9]A. B. Fowler and A. M. Hartstein, Surf. Sci. **98**, 169 (1980).
[10]D. J. Thouless, Phys. Rep. **13C**, 93 (1974).
[11]J. M. Ziman, *Models of Disorder* (Cambridge University Press, Cambridge, 1979).
[12]N. F. Mott, Adv. Phys. **16**, 49 (1967).
[13]F. F. Fang, A. B. Fowler, and A. Hartstein, Phys. Rev. B **16**, 4446 (1977).
[14]J. P. Harrang, R. K. Goodall, and R. J. Higgins, Bull. Am. Phys. Soc. **29**, 472 (1984).
[15]T. Ando and Y. Uemura, J. Phys. Soc. Jpn. **36**, 959 (1974).
[16]J. Wakabayashi, H. W. Myron, and M. Pepper, Physica **117B—118B**, 691 (1983).
[17]M. A. Paalanen, D. C. Tsui, and A. C. Gossard, Phys. Rev. B **25**, 5566 (1982).
[18]K. von Klitzing, Festkörperprobleme **XXI**, 1 (1981).
[19]Roger Haydock (private communication); this is implicit in the Kubo formalism and reflected in the calculations of Ando.
[20]F. F. Fang and P. J. Stiles, Phys. Rev. **174**, 823 (1968).
[21]T. Ando and Y. Uemura, J. Phys. Soc. Jpn. **37**, 1044 (1974).
[22]H. Lefevre (private communication).
[23]This was initially done to increase the strength of the capacitance structure. The modified boundary conditions effectively double α.
[24]Y. Imry, J. Phys. C **15**, L221 (1982).